FIELD FORMATION IN CYCLOTRON CC18/9

Abstract

Results of field formation are presented for the small cyclotron CC18/9 designed for the ABO University clinic (Turku, Finland) and Central Radiological Institute (St.Petersburg, Russia). CC18/9 is intended for proton/deuteron acceleration. Desired isochronous field was obtained by iterative solving a self-consistent problem on the basis of precise 3D field simulations with the use of the software package KOMPOT. A detailed calculation of an original shimming system was performed. The system was optimised using magnetic measurements. A comparison between the calculated and measured data is presented.

Cyclotron CC18/9 has been designed for the ABO University clinic (Turku, Finland) and Central Radiological Institute (St.Petersburg, Russia) and is used for proton/deuteron acceleration. This paper presents results of the field formation in CC18/9 based on numerical modelling. Details of the numerical method applied to form a desired field distribution with the use of 3D KOMPOT [1] modelling are presented in Ref. [2], [3].

The numerical procedure of the CC12 field formation included the following main stages.

1. At the initial stage basic parameters of the magnet system were determined from the magnetooptic calculations.

2. The second stage involved the development of a realistic 3D model for the DC60 magnet system. The model used detailed descriptions of the magnet geometry, media interfaces, and non-linear properties of steel. For initial calculations a standard near-realistic B-H curve was used as reference. Then steel properties were corrected using the results of magnetic measurements on samples of steel used in the fabrication of the magnet. The curves $B(H),\ \mu(H),\ \mu(B),\ \partial\mu/\partial H$) obtained for the real magnet were used to simulate the expected field distribution and to choose the shimming method. Figures 1,2 present a part of the finite-element model of CC12 magnet system (magnetic circuit and coils only). The model covers a 1/16 of the magnet system and includes boundary conditions with respect to the magnet symmetry. The external boundary for the calculated region was taken so that to avoid the influence of the boundary conditions on the field behaviour inside the working zone and type of field decay with distance from the magnet. The finite-element mesh has about 180000 nodes.

3. Разработанная вычислительная модель использовалась для предварительного анализа пространственного поля. Магнито-оптический анализ позволил определить требуемые изохронные зависимости для ускорения протонов и дейтонов. На последующем шаге в разработанную модель вносились различные геометрические изменения с целью расчета функций влияния [2] различных конструктивных элементов и выбора способа формирования поля. В результате проведенного анализа в качестве основного метода формирования поля в установке CC18/9 было выбрано азимутальное шиммирование боковой поверхности секторов. Для перестройки поля при переходе с одного типа частиц на другой был выбран подвижной азимутально-профилированный шимм, расположенный в полости внутри сектора и перемещающийся в радиальном направлении. The finite-element model was applied to preliminary analyse a spatial field distribution. From the magnetooptic analysis required isochronous curves was found to provide proton and deuterion acceleration. The next step was to vary geometrical parameters in order to calculate the influence functions [2] for different magnet components and select the shimming method. From the results of the calculation, the azimuthal shimming by shaping the sector sides was chosen to form a desired field distribution.

4. The influence functions obtained were used to form a required isochronous field to provide both proton (shim moved in) and deuterion (shim moved out) acceleration regimes.

Figures 3,4 show calculated field distributions over typical cross sections for the optimised magnet configuration. Figure 5 shows an averaged field distribution in the reference and optimised magnet system in comparison with the desired isochronous field. The required isochronous field was formed in two stages. At the first stage an isochronous field required to accelerate protons was formed by shaping the sector sides, the movable shim being pushed inside. At the second stage the movable shim was pushed out, and an isochronous field required to accelerate deutons was formed by adjusting the shim side profile. At each stage the field was iteratively optimised. Each iteration had a prediction phase and a correction phase. During the prediction phase the magnet geometry was varied slightly, and a new magnet circuit configuration was formed from the field distribution of the previous iteration and known influence functions having regard to the required isochronous curve. In the correction phase, a field distribution was calculated for the obtained magnet configuration taking into account the saturation effect. After several iterations, the trajectory analysis was performed on the basis of the generated field map to correct the isochronous curve and to close the solution of the self-consistent problem. If the iterated geometry differed markedly from the reference configuration, the influence functions were re-calculated.

The proposed numerical method allowed effective field formation in CC18/9 taking into consideration realistic properties of steels used in the fabrication. The influence function obtained made it possible to estimate manufacture/assembly tolerances, which will be used for magnetic measurements and magnet adjustment.

References

[1] *Program package for 3D simulation of stationary magnetic fields, analysis and synthesis of magnet system for electrophysical devices (KOMPOT/M 1.0).* Registration Certificate # 2003612492 of Nov.12, 2003. Computer program register, Moscow

[2] A.Belov, V.Belyakov, T.Belyakova et al. *KOMPOT 3D field simulations for cyclotron magnet systems* // ICAA Proc., this issue

[3] Gulbekian G.G et al. *The method of the magnetic field formation in cyclotron DC-72.* Nukleonika 48(4), 2003, pp.207-210.

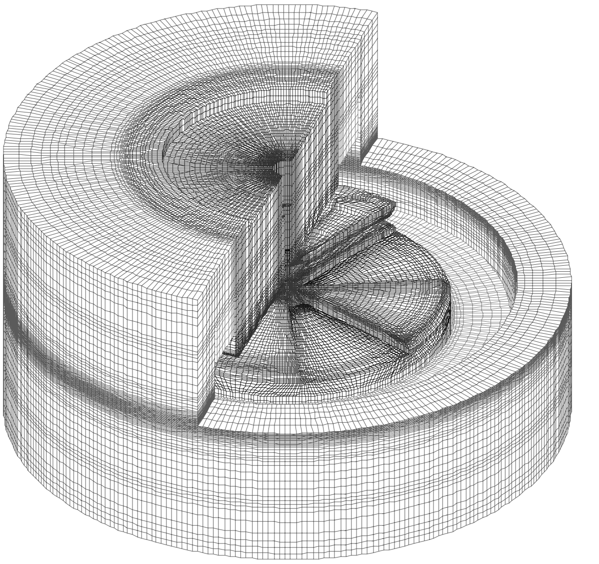

Fig.1. Finite-element model of CC18/9 magnet system

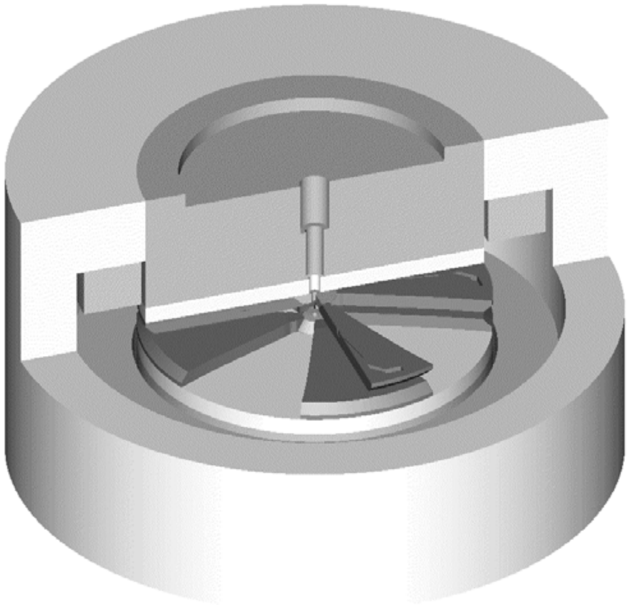

Fig.2. CC18/9 solid geometry generated from FE model

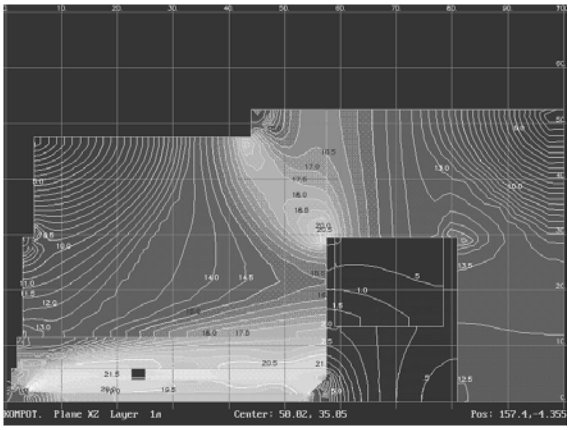

Fig.3. Simulated field map in CC18/9 vertical plane

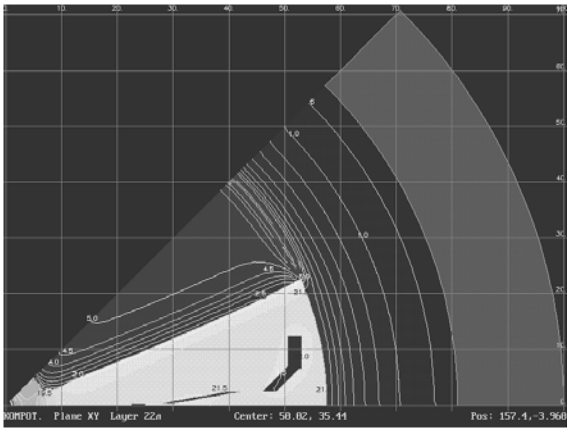

Fig.4. Simulated field map in CC18/9 horisontal plane across sector

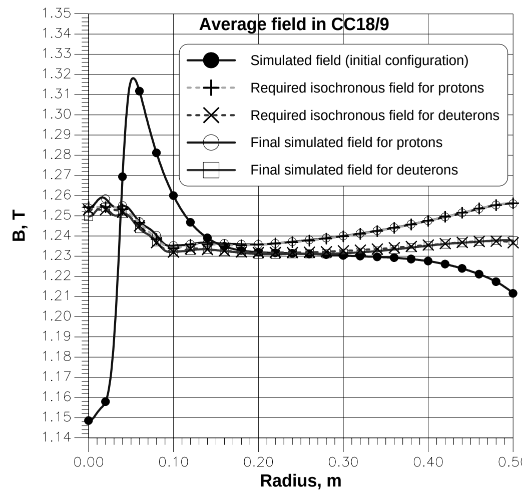

Fig.5. Averaged field variations with radius